

Constraints on $U(1)_{L_\mu-L_\tau}$ from LHC Data

Manuel Drees¹, Meng Shi² and Zhongyi Zhang³

Physikalisches Institut and Bethe Center for Theoretical Physics,
Bonn University, 53115 Bonn, Germany

In this study, we apply LHC data to constrain the extension of the Standard Model by an anomaly-free $U(1)_{L_\mu-L_\tau}$ gauge group; this model contains a new gauge boson (Z') and a scalar dark matter particle (ϕ_{DM}). We recast a large number of LHC analyses of multi-lepton final states by the ATLAS and CMS collaborations. We find that for $10 \text{ GeV} < m_{Z'} < 60 \text{ GeV}$ the strongest constraint comes from a dedicated Z' search in the 4μ final state by the CMS collaboration; for larger Z' masses, searches for final states with three leptons plus missing E_T are more sensitive. Searches for final states with two leptons and missing E_T , which are sensitive to Z' decays into dark matter particles, can only probe regions of parameter space that are excluded by searches in the 3 and 4 lepton channels. The combination of LHC data excludes values of Z' mass and coupling constant that can explain the deficit in $g_\mu - 2$ for $4 \text{ GeV} \leq m_{Z'} \leq 500 \text{ GeV}$. However, for much of this range the LHC bound is weaker than the bound that can be derived from searches for “trident” events in neutrino–nucleus scattering.

¹drees@th.physik.uni-bonn.de

²mengshi@physik.uni-bonn.de

³zhongyi@th.physik.uni-bonn.de

1 Introduction

There are several reasons for considering the extension of the gauge group of the Standard Model (SM) by another Abelian $U(1)$ factor. It is usually assumed that the new gauge boson couples universally to all three generations of quarks, in order to avoid constraints from flavor-changing neutral currents. If we further insist that the gauge group should be anomaly-free within the SM matter content (possibly extended by right-handed neutrinos, but without other exotic chiral fermions), there are only four different possibilities. These can be written as $B - L$ [1], as well as the purely leptonic $L_e - L_\mu$, $L_\mu - L_\tau$, and $L_e - L_\tau$ [2]; of course, linear combinations of these four groups are also possible. In the $U(1)_{B-L}$ model, which does require right handed neutrinos, the new gauge boson couples to both quarks and (charged) leptons. This model is therefore tightly constrained by searches for di-lepton resonances at hadron colliders, in particular at the LHC [3, 4]; if the coupling of the new $U(1)$ is comparable to that of the $U(1)_Y$ of the SM, these searches exclude Z' masses below several TeV.*

In the other three models the cancellations of anomalies occur between different generations without the requirements of extra fermions [2]. LEP data strongly constrain the $L_e - L_\mu$ and $L_e - L_\tau$ models. While we are not aware of dedicated analyses of LEP data in the framework of these models, for $m_{Z'} > 300$ GeV or so the Z' propagator at LEP energies ($\sqrt{s} \leq 209$ GeV) can be approximated by a constant, in which case limits on contact interactions apply. In particular, ALEPH data on $e^+e^- \rightarrow \mu^+\mu^-$ [6] imply $m_{Z'}/g_{e\mu} > 1.1$ TeV for the $L_e - L_\mu$ model, whereas OPAL data on $e^+e^- \rightarrow \tau^+\tau^-$ [7] lead to the bound $m_{Z'}/g_{e\tau} > 0.94$ TeV for the $L_e - L_\tau$ model. For smaller Z' masses, where propagator effects become important, the bound will be even stronger.

In contrast, the $L_\mu - L_\tau$ model does not predict any new interaction for the electron. Its gauge boson can therefore only be produced through higher-order processes in e^+e^- collisions, by emission off a charged or neutral lepton of the second or third generation. These final states can also be produced at the LHC [8], which has accumulated a far larger number of di-muon and di-tau events than LEP did. In this paper we therefore focus on LHC data. Note also that the $U(1)_{L_\mu - L_\tau}$ model can accommodate successful neutrino masses even with the simplest Higgs sector [9, 10], and can be extended to contain a dark matter particle that is charged under the new symmetry but easily satisfies the stringent direct search constraints [11, 12]. In principle, this model could also explain the difference between SM prediction and measurement of the anomalous magnetic moment of the muon ($g_\mu - 2$); however, bounds on $\nu_\mu N \rightarrow \nu_\mu \mu^+ \mu^- N$ “trident” production [13], where N stands for some nucleus, exclude this possibility for $m_{Z'} > 0.5$ GeV.

The other existing constraint in the Z' mass range relevant for searches at the LHC comes from analyses of Z decays into four charged leptons [17]. In particular, ref. [18] is a CMS analysis constraining this model using $Z \rightarrow 4\mu$ decays. This search is obviously only sensitive to relatively light Z' , $m_{Z'} < m_Z$. LHC prospects for this model have been discussed previously [14–16], with ref. [16] focussing on the case $m_{Z'} \leq m_Z/2$; however, these papers did not attempt to use actual LHC data to constrain the model.

In contrast, we consider a comprehensive set of LHC analyses for final states with two, three or four charged leptons in the final state, where a lepton l for us means a muon or a hadronically decaying τ . Final states with fewer than four charged leptons are also re-

*See ref. [5] for a very recent assessment on current constraints on the $B - L$ model.

quired to contain some missing transverse momentum $E_T^{\cancel{e}}$. In particular, final states with only two charged leptons plus $E_T^{\cancel{e}}$ are sensitive to Z' decays into dark matter particles, which also reduce the branching ratios for Z' decays into μ or τ pairs. $\tau \rightarrow \mu$ decays contribute to muonic final states, if typically with reduced efficiency since the muon produced in τ decays is obviously softer than the parent τ . In principle, $\tau \rightarrow e$ decays can also populate final states with electrons. However, the small branching ratio (about 18%) and again reduced efficiency imply that final states with electrons will not be as sensitive as those only containing muons or hadronically decaying τ leptons. We use the CheckMATE framework [19, 20]. Only a few of the analyses we applied had already been included in CheckMATE. We included a total of 281 new signal regions defined in 28 different papers.[†] We find that the specialized Z' search [18] based on 4μ final states is indeed most sensitive for $10 \text{ GeV} \leq m_{Z'} \leq 60 \text{ GeV}$; for larger masses, analyses of final states containing only three charged leptons are more sensitive.

The full $SU(3)_c \times SU(2)_L \times U(1)_Y \times U(1)_{L_\mu-L_\tau}$ model introduced in [11, 12] contains not only the new mediator and DM particle, but also an extra Higgs boson to break the new $U(1)$ as well as SM singlet right-handed neutrinos for a see-saw generation of realistic neutrino masses. The extra Higgs boson plays a significant role in the dark matter phenomenology, but it can contribute to the final states we consider only if its mixing angle with the $SU(2)$ doublet Higgs boson responsible for electroweak symmetry breaking is relatively large. We ignore this possible source of additional signal events. The main free parameters are thus the mass of the Z' and the strength of its coupling to μ and τ leptons; the branching ratio for Z' decays into dark matter particles also plays a (lesser) role.

The remainder of this Letter is organized as follows. In Sec. 2, we briefly describe the parts of the $U(1)_{L_\mu-L_\tau}$ model [11, 12] that are relevant for the LHC searches we consider. The application to LHC data is discussed in Sec. 3, both for vanishing and non-vanishing branching ratio for Z' decays into dark matter particles. Finally, Sec. 4 contains our summary and conclusions.

2 The Simplified $U(1)_{L_\mu-L_\tau}$ Model

The $SU(3)_c \times SU(2)_L \times U(1)_Y \times U(1)_{L_\mu-L_\tau}$ model contains a new gauge boson Z' for the local $U(1)_{L_\mu-L_\tau}$ symmetry; the corresponding field strength tensor is $\mathcal{Z}'_{\mu\nu} \equiv \partial_\mu Z'_\nu - \partial_\nu Z'_\mu$. As usual, we write its interaction with other particles using the covariant derivative instead of the normal partial derivative, i.e. $\partial_\mu \rightarrow D_\mu = \partial_\mu - ig_{\mu\tau} q Z'_\mu$, where $g_{\mu\tau}$ is the new gauge coupling and q is the $L_\mu - L_\tau$ charge of the particle in question. The model also contains a complex scalar ϕ_{DM} , which is singlet under the gauge group of the SM but carries $L_\mu - L_\tau$ charge q_{DM} . The new part of the complete Lagrangian that is relevant for our analysis is thus given by

$$\begin{aligned} \mathcal{L}_{\text{new}} = & (D_\mu \phi_{\text{DM}})^* D^\mu \phi_{\text{DM}} - m_{\text{DM}}^2 \phi_{\text{DM}}^* \phi_{\text{DM}} - \frac{1}{4} \mathcal{Z}'_{\mu\nu} \mathcal{Z}'^{\mu\nu} + \frac{1}{2} m_{Z'}^2 Z'^\mu Z'_\mu \\ & + g_{\mu\tau} (\bar{\mu} \cancel{Z}'^\mu \mu + \bar{\nu}_\mu \cancel{Z}'^\mu \nu_\mu - \bar{\tau} \cancel{Z}'^\mu \tau - \bar{\nu}_\tau \cancel{Z}'^\mu \nu_\tau). \end{aligned} \quad (1)$$

[†]Most of the experimental papers we used also include signal regions containing electrons. We did not consider those, for the reasons explained above. By current policy an analysis can become part of the official CheckMATE release only if all of the signal regions defined in this analysis are encoded. Our “private” version of CheckMATE is available upon request.

The LHC signals we consider originate from the production and decay of (nearly) on-shell Z' bosons. At leading order the Z' can only decay into second or third generation leptons, and possibly into DM particles. The corresponding partial widths are given by

$$\Gamma(Z' \rightarrow l^+l^-) = \frac{g_{\mu\tau}^2 m_{Z'}}{12\pi} \sqrt{1 - 4z_l}(1 + 2z_l), \quad \text{for } l = \mu, \tau; \quad (2)$$

$$\Gamma(Z' \rightarrow \phi_{\text{DM}}\phi_{\text{DM}}^*) = \frac{q_{\text{DM}}^2 g_{\mu\tau}^2 m_{Z'}}{48\pi} (1 - 4z_{\text{DM}})^{3/2}, \quad (3)$$

where $z_X \equiv \frac{m_X^2}{m_{Z'}^2}$. The partial width for Z' decays into one flavor (μ or τ) of neutrino is half of that given in eq.(2), since only the left-handed neutrinos are light enough to contribute. In our analysis we only consider scenarios where the total Z' width is smaller than $m_{Z'}$, since otherwise perturbation theory is not reliable. This translates into the condition

$$q_{\text{DM}}^2 (1 - 4z_{\text{DM}})^{3/2} + 4 \sum_{l=\mu, \tau} \sqrt{1 - 4z_l}(1 + 2z_l) + 4 < 48\pi/g_{\mu\tau}^2. \quad (4)$$

This bound is always satisfied for $g_{\mu\tau} \leq 3$ and $q_{\text{DM}} \leq 2$.

3 Application to LHC Data

At tree-level the only SM particles our Z' boson couples to are leptons of the second and third generation. These can be pair-produced via neutral or charged current Drell-Yan processes. The leading-order Z' production processes are based on these Drell-Yan reactions, with a Z' boson being emitted off the lepton line, see Fig. 1.

If the primary Drell-Yan process produces an l^+l^- pair (left diagram), $Z' \rightarrow l'^+l'^-$ decays lead to final states containing four charged leptons, where flavor l' may be the same or different from l (with $l, l' \in \{\mu, \tau\}$). Invisible Z' decays, into neutrinos or DM particles, lead to final states with an opposite-sign same-flavor charged lepton pair plus missing E_T .

If the primary Drell-Yan reaction produces a $\nu_l\bar{\nu}_l$ pair (middle diagram), Z' decays into charged leptons again lead to $l^+l^- E_T$ final states. For this production process invisible Z' decays do not result in a detectable final state.*

Finally, if the primary Drell-Yan reaction produces a $l^-\bar{\nu}_l$ pair or its charge conjugate (right diagram), Z' decays into charged leptons leads to final states of the type $l^\pm l'^+ l'^- E_T$, where the l and l' may again be the same or different flavors. In this case invisible Z' decays lead to final states with a single charged lepton plus missing E_T . This can be considered a higher-order correction to the SM charged-current Drell-Yan reaction, and will certainly have a far worse sensitivity than the $3l + E_T$ final state.

Of course, experimentally a μ and a τ look very different. In fact, primary muons and muons from tau decays cannot be distinguished reliably; we will just add these contributions. For reasons described in the Introduction, we do not consider final states containing electrons, which might be produced in tau decays. However, we do consider final states including hadronically decaying tau leptons, which we denote by τ_h .

*If a hard parton is emitted off the initial state this process would contribute to monojet production; however, it would merely be a higher-order correction to monojet production in the SM, and would thus certainly not lead to a detectable signal.

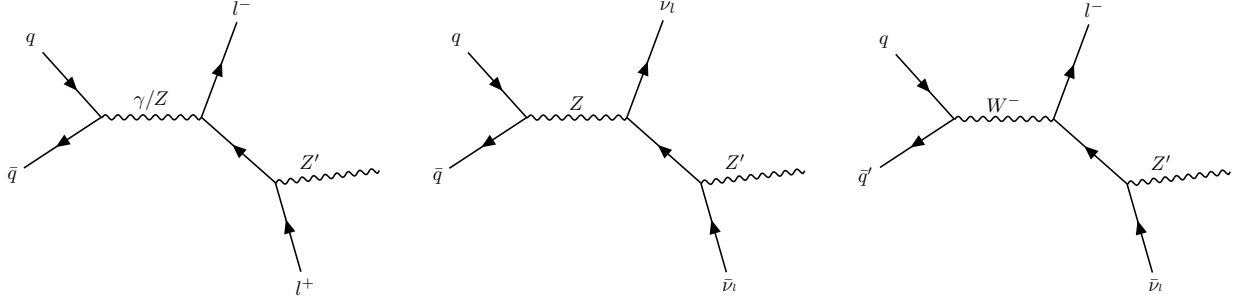


Figure 1: Examples of Feynman diagrams for $pp \rightarrow Z'l^+l^-$ (left), $pp \rightarrow Z'\nu_l\bar{\nu}_l$ (center) and $pp \rightarrow Z'l\nu_l$ (right). For the left diagram, both visible (leptonic) and invisible Z' decays (into neutrinos or DM particles) contribute to signal processes, but for the central and right diagram only Z' decays into a charged lepton pair were considered. The Z' boson can also be emitted off the other lepton, and W^+ exchange diagrams also contribute. In the event generation the Z' is allowed to be off-shell.

Altogether, we thus consider the following distinct final states: 3μ , 4μ , $m\mu + n\tau_h$ ($m+n > 2$, $n \neq 0$), $2\tau_h + E_T$, $\mu\tau_h + E_T$, and $2\mu + E_T$. The corresponding LHC analyses we recast are summarized in Table 1. To that end we used the CheckMATE 2 framework [20], which in turn uses Delphes 3 [21] to simulate the CMS [22] and ATLAS [23] detectors. It should be noted that CheckMATE also uses several other public tools [21, 24–34]. As mentioned in the Introduction, we encoded a total of 281 new signal regions; we also used a few searches for superparticles in multi-lepton final states which had already been included in CheckMATE.

List of Analyses	Center-of-mass energy		
	7 TeV	8 TeV	13 TeV
Topologies			
$2\mu + E_T$	[35, 36]	[35, 37–39]	[4, 40–49]
$(2\tau_h \text{ or } \mu\tau_h) + E_T$			[50–53]
$3\mu \text{ or } 4\mu$		[54]	[18, 44, 45, 48, 49, 55–61]
$m\mu + n\tau_h$ ($m+n > 2$, $n \neq 0$)		[62]	[44, 56, 60, 61]

Table 1: All analyses used in this study.

In order to simulate the signal, we used FeynRules [63] to produce a model file output in UFO format [64]. Parton-level events were generated by MadGraph [65]. Specifically, we defined charged leptons (meaning μ^- and τ^-) and invisible particles (μ and τ neutrinos or antineutrinos as well as DM particles). The $2l$ signal events were generated by specifying MadGraph events containing a charged lepton–antilepton pair plus two missing particles; for the $3l$ signal, MadGraph generated events with three charged leptons and one missing particle; and the $4l$ signal started from MadGraph-generated events with two pairs of charged leptons. In all cases only diagrams containing one Z' propagator (i.e. two new couplings) were generated.

This means that the Z' boson is allowed to be off-shell, but interference between Z' and Z or photon exchange is not included. These interference terms formally vanish in the nar-

row width approximation, i.e. for $\Gamma_{Z'} \rightarrow 0$. These terms are therefore expected to be more important for larger coupling $g_{\mu\tau}$, which in turn are allowed for larger $m_{Z'}$, as discussed quantitatively below. However, we found that even for the largest coupling we consider, which respects the perturbativity constraint (4), the interference contribution to the cross section after cuts is at most 6% of the squared Z' exchange contribution. This is considerably less than the effect of typical QCD NLO corrections, which we also ignore. Note also that in the high mass region ($m_{Z'} > 100$ GeV), where the upper limit of $g_{\mu\tau}$ is sizable and considered offering noticeable interference contribution, we found the interference terms to be positive, so ignoring them is conservative.

These MadGraph events were passed on to Pythia 8.2 [66] for parton showering and hadronization, and then to CheckMATE 2 [20] which applies the selection cuts defined by the designated search regions and decides whether the given model is excluded by these searches or not.

We performed separate comparisons to $2l$, $3l$ and $4l$ searches; we remind the reader that l here means a muon or a hadronically decaying τ lepton. Some of the analyses we apply used data taken at $\sqrt{s} = 7$ or 8 TeV, which required separate event generation. However, at the end the analyses of data taken at $\sqrt{s} = 13$ TeV, many of which were published quite recently, always proved more constraining. Moreover, we find that replacing a muon in the final state by a hadronically decaying τ always reduces the sensitivity. The branching ratio for hadronic τ decays is about 65%, but the τ -tagging efficiency is well below the efficiency of identifying a muon, and QCD jets are much more likely to be misidentified as a hadronically decaying τ than as a muon. Nevertheless τ leptons do contribute to the final sensitivity, through $\tau \rightarrow \mu$ decays.

In the following we will present constraints on the $L_\mu - L_\tau$ gauge boson in two different scenarios. We begin with scenarios where the Z' boson does not decay into dark matter particles, either because $q_{\text{DM}} = 0$ or because $m_{\text{DM}} > m_{Z'}/2$. The strengths of all signals we consider can then be computed uniquely in terms of only two parameters: the mass $m_{Z'}$ and the coupling $g_{\mu\tau}$. We generate at least 20,000 events for each combination of Z' mass and coupling; if the total error in the most relevant signal region is dominated by Monte Carlo statistics, we generate additional events. Since the signal rates to good approximation scale like $g_{\mu\tau}^2$, we typically only need to try three to four values of the coupling in order to determine its upper bound for a given value of $m_{Z'}$.

In the left frame of Fig. 2 we show upper bounds on $g_{\mu\tau}$ that have been derived in this manner as functions of $m_{Z'}$. The figure shows separate bounds from analyses of final states with two (green dot-dashed curve), three (red dashed curve) and four (dark blue solid curve) charged leptons. The right frame shows the upper bounds on the corresponding total cross sections, which include the branching ratios for Z' decays but count each τ as a charged leptons, irrespective of its decay. The curves terminate in the region of large Z' mass when the perturbativity limit (4) is reached. The curves aren't always smooth. The reason is that CheckMATE uses the signal region with the best expected sensitivity to set the bounds. This avoids “look elsewhere” effects, but can lead to discontinuities when the relevant signal region changes. Finally, we do not show bounds from $2l$ final states for $m_{Z'} < 10$ GeV since the cut efficiency becomes very poor there, i.e. we would need to generate a very large number of events in order to derive reliable results; we did not do that since the resulting bound will surely again be worse than that from $3l$ and $4l$ analyses.

The left frame also shows the value of $g_{\mu\tau}$ where the full theory prediction, including Z' exchange, reproduces the measured value of $g_\mu - 2$. The brown solid line corresponds to

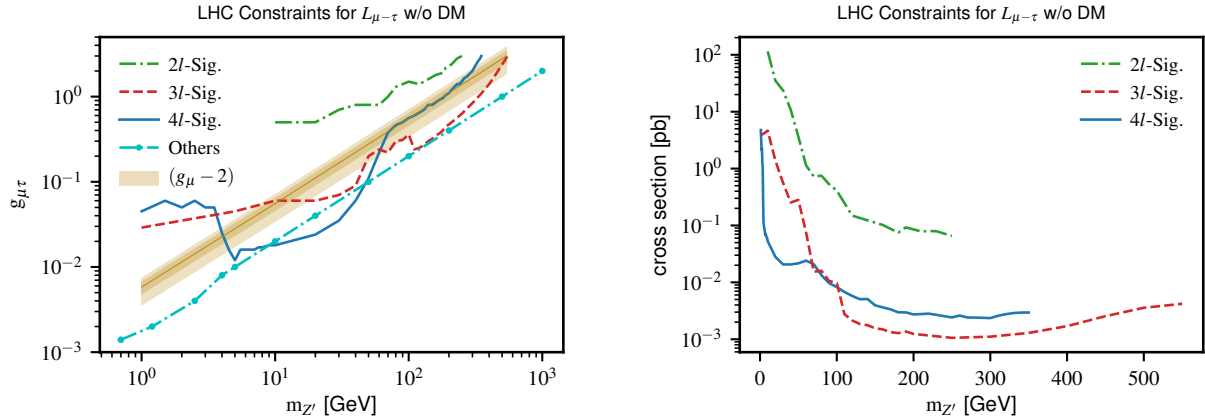


Figure 2: The upper limit on the new coupling $g_{\mu\tau}$ (left) and the corresponding cross section before cuts (right). The left frame also shows the value of the coupling indicated by the measurement of the anomalous magnetic moment of the muon (shaded area), as well as a summary of existing constraints (lower dot-dashed curve); see the text for further details.

the central value, whereas the darker and lighter shaded regions allow too reproduce $g_{\mu} - 2$ up to 1 and 2 standard deviations, respectively. Here we use

$$\Delta a_{\mu} = a_{\mu}^{exp} - a_{\mu}^{th} = (29.0 \pm 9.0) \times 10^{-10}$$

from [67], which is was also used in the non-collider studies [11,12] we discussed previously.

Finally, the lower dot-dashed line in the left frame summarizes non-LHC bounds. For $m_{Z'} > 4$ GeV the results from non-LHC data come from our interpretation of the CCFR measurement of the cross section for “trident” production [68]. We used the CL_S method to set the 95% c.l. limit, which is also employed by CheckMATE. The resulting bound on $g_{\mu\tau}$ is $\sim 20\%$ weaker than that derived by taking the central value of the CCFR cross section plus 1.64 times the CCFR error as upper bound on the cross section, which seems to have been done in [13]; note that the cross section measured by CCFR is somewhat below the SM prediction.[†] For $m_{Z'} < 4$ GeV the best non-LHC bound comes from 4μ searches by the BaBar collaboration [70]. We show a smoothed-out version of the actual bound, which fluctuates rapidly by $\sim \pm 30\%$ around this line. In [71] it was shown that bounds from tests of lepton universality are always weaker than that from the neutrino trident experiments in the parameter region we focus on ($m_{Z'} \leq 500$ GeV). We therefore do not show these constraints in Fig. 2.

As mentioned above, there is only one published analysis of LHC data that specifically searches for the $L_{\mu} - L_{\tau}$ gauge boson [18]; it covers the mass range $5 \text{ GeV} < m_{Z'} < 70$ GeV using $Z \rightarrow 4\mu$ decays in the CMS detector. Our CheckMATE based recast of this analysis leads to a similar, but slightly weaker constraint on $g_{\mu\tau}$ for given $m_{Z'}$; this difference presumably results from inaccuracies of the fast Delphes 3 simulation of the CMS detector, as compared to the full simulation based on Geant 4 [72] employed by the CMS collaboration. For Z' masses between 10 and 60 GeV, this search provides the strongest bound of all LHC searches.

[†]The CHARM-II collaboration also measured this cross section, with a different neutrino beam, and found a result somewhat larger than, but compatible with, the SM prediction [69]. Naively averaging the two measurements of σ_{exp}/σ_{SM} leads to a very similar bound on $g_{\mu\tau}$ when using the CL_S method.

However, outside this mass range the tightest LHC constraint comes from other searches. In particular, for $m_{Z'} < 10$ GeV the 4μ search in [61], which includes softer muons, is comparable to or sometimes stronger than [18]. On the other hand, for $m_{Z'} > 60$ GeV the best LHC bound comes from searches for 3μ final states, the most important ones being [55] and, for $m_{Z'} > 100$ GeV, [61]. Another analysis [44] uses the same selection rules as [61] with different categorization, and thus gives similar results. The main reason for the good performance of the 3μ searches is that the cross section for the charged current Drell–Yan process is larger by a factor of 2.5 to 3 than that for the corresponding neutral current process leading to a charged lepton pair; this relative ordering is not affected much by the Z' boson emitted off the leptons line (see Fig. 1) [8]. Moreover, the cut efficiency for the most sensitive 3μ analysis turns out to be a little better.

On the other hand, Fig. 2 also shows that the LHC bounds are stronger than existing constraints only in the mass range covered by the dedicated search [18]. Note also that the upper bounds on the signal cross sections flatten out, or even slightly increase, at large Z' masses (right frame). This is a sure sign that the cuts were not optimized for the $L_\mu - L_\tau$ model. For example, the upper bound derived from 3μ final states in [61] increases at large $m_{Z'}$ largely because of a transverse mass cut, which loses efficiency.

So far we have assumed that DM particles cannot be produced in on-shell Z' decays. If we allow $Z' \rightarrow \phi_{\text{DM}}\phi_{\text{DM}}^*$ decays the branching ratio for $Z' \rightarrow l^+l^-$ decays will be reduced, leading to reduced $3l$ and $4l$ signals. However, since we consider a scalar DM particle, even for $q_{\text{DM}} = \pm 2$ the branching ratio for Z' decays into DM particles does not exceed 25%. This would reduce the upper bounds on $g_{\mu\tau}$ derived from these channels by a factor of at most $\sqrt{12}/4 \simeq 0.86$.

The situation for the $2l$ channel is different. The contribution from the left Feynman diagram in Fig. 1 to this final state increases with increasing branching ratio for invisible Z' decays, while that from the middle diagram decreases. Since for $|q_{\text{DM}}| \leq 2$ the branching ratio for invisible Z' decays is never more than 50%, one might expect the former effect to be dominant; however, the two diagrams have both different total cross sections and different cut efficiencies, making a numerical analysis necessary.

Some results are shown in Fig. 3, for $g_{\mu\tau} = 1$ and $q_{\text{DM}} = 1$ (left) and 2 (right). The green regions are excluded by our recast of analyses of 2μ final states; the corresponding exclusion limits in the absence of $Z' \rightarrow \text{DM}$ decays are given by the horizontal black lines. The fact that the green regions extend beyond the upper horizontal line shows that allowing $Z' \rightarrow \phi_{\text{DM}}\phi_{\text{DM}}^*$ decays increases the sensitivity of this final state somewhat, the effect being slightly bigger for $q_{\text{DM}} = 2$. The strongest bounds are from three different analyses of data taken at $\sqrt{s} = 13$ TeV [43, 45, 47], and their cut efficiencies are indeed quite different for $pp \rightarrow Z'\nu_l\bar{\nu}_l$ and $pp \rightarrow Z'l\bar{l}$ processes. However, this entire region of parameter space is still excluded by analyses of final states with three or four muons. Therefore LHC data are not sensitive to the production of dark matter particles in this model.

So far we have considered a complex scalar as dark matter candidate. However, in on-shell Z' decays the spin of invisible particles cannot be determined; the only quantity relevant for LHC analyses is the invisible branching ratio of the Z' boson. For example, we could just as well consider a Dirac fermion χ as dark matter candidate. The relevant partial width would then be given by

$$\Gamma(Z' \rightarrow \bar{\chi}\chi) = \frac{m_{Z'}}{12\pi} \sqrt{1 - 4z_{\text{DM}}} (g_V^2 + g_A^2 + 2z_{\text{DM}}(g_V^2 - 2g_A^2)), \quad (5)$$

where the g_A is the axial vector coupling, g_V is the vector coupling, and $z_{\text{DM}} = m_\chi^2/m_{Z'}^2$.

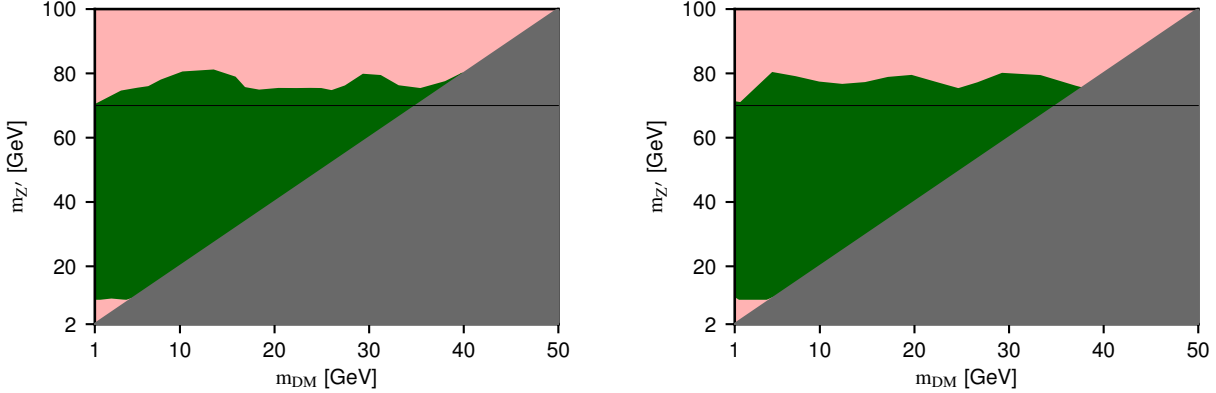


Figure 3: The effect of Z' decays into dark matter particles on the constraint from $2l$ final states, for $g_{\mu\tau} = 1$ and $q_{\text{DM}} = 1$ (left) and 2 (right). In the gray region below the diagonal these decays are kinematically forbidden, i.e. the result of Fig. 2 holds. The green region is excluded by analyses of 2μ final states at $\sqrt{s} = 13$ TeV; in the absence of $Z' \rightarrow \text{DM}$ decays these analyses exclude the region between the horizontal lines. The pink region is excluded by analyses of 4μ final states, which are only mildly affected by $Z' \rightarrow \text{DM}$ decays; this includes the entire green region.

For $g_V = 0$ and $g_A = g_{\mu\tau}$, this partial width is the same as that for scalar DM for $q_{\text{DM}} = 2$ shown in the right frame of Fig. 3. On the other hand, for $g_A = 0$ and $g_V = g_{\mu\tau}$, eq.(5) predicts a somewhat larger partial width for sizable mass of the DM particle. However, the branching ratio for Z' decays into dark matter still remains below 25%, and the constraints from $2\mu + \cancel{E}_T$ searches remain far weaker than those from analyses of final states with 3 or 4 muons.

4 Conclusions

In this study, we recast a large number of LHC analyses, summarized in Table 1, from both the CMS and ATLAS collaborations in the CheckMATE framework in order to constrain the $U(1)_{L_\mu-L_\tau}$ extension of the SM. Here we focus on the new Z' gauge boson predicted by this model, whose mass and coupling are the main free parameters relevant for LHC physics. We find that recently published analyses of data taken at $\sqrt{s} = 13$ TeV always have higher sensitivity than LHC data taken at lower energies. These data exclude Z' masses up to 550 GeV for perturbative couplings. We analyzed final states containing two, three or four charged leptons, where a charged lepton is here defined as a muon or a hadronically decaying τ lepton. Final states with only two charged leptons in principle would have the highest sensitivity to Z' decays into invisible dark matter particles, but this final state is always much less sensitive than the $3l$ and $4l$ final states. Moreover, replacing a muon by a hadronically decaying τ lepton always reduced the sensitivity. The final LHC limit is therefore set by 4μ final states for $5 \text{ GeV} < m_{Z'} < 60 \text{ GeV}$, and by 3μ final states otherwise. However, except for $10 \text{ GeV} < m_{Z'} < 60 \text{ GeV}$ LHC data are still no more sensitive to this model than data taken at much lower energies, in particular analyses of $\nu_\mu N \rightarrow \mu^+ \mu^- N$ “trident” production by the CCFR collaboration [68].

Only one analysis we use [18], which looks for $Z \rightarrow 4\mu$ decays, has been designed specifically for this Z' boson. It is thus very likely that the sensitivity could be enhanced, in particular for larger Z' masses, by optimizing the cuts, in particular in 3μ final states which have a larger cross section before cuts. A further increase of sensitivity might be possible by statistically combining final states with muons and with hadronically decaying τ leptons, since the relative normalization of these channels can be predicted unambiguously in this model; for example, for $m_{Z'} \geq 10$ GeV, where lepton mass effects are negligible, the branching ratios for Z' decays into $\mu^+\mu^-$ and $\tau^+\tau^-$ are essentially the same.

In this paper we focused on the production of the new Z' gauge boson. The model also contains a new Higgs boson, which may decay via two real or virtual Z' bosons into up to four charged leptons. Both the decay of the 125 GeV Higgs boson into two of the new Higgs bosons, and the emission of the new Higgs boson off a Z' boson in one of the diagrams of Fig. 1, can therefore lead to spectacular final states with up to eight charged leptons. We leave their investigation to future work.

ACKNOWLEDGEMENTS

This work was partially supported by the by the German ministry for scientific research (BMBF). Meng Shi was supported by the China Scholarship Council (grant no. 201606100045).

References

- [1] Rabindra N. Mohapatra and R. E. Marshak. Local B-L Symmetry of Electroweak Interactions, Majorana Neutrinos and Neutron Oscillations. *Phys. Rev. Lett.*, 44:1316–1319, 1980. [Erratum: *Phys. Rev. Lett.*44,1643(1980)].
- [2] X. G. He, Girish C. Joshi, H. Lew, and R. R. Volkas. NEW Z-prime PHENOMENOLOGY. *Phys. Rev.*, D43:22–24, 1991.
- [3] Morad Aaboud et al. Search for new high-mass phenomena in the dilepton final state using 36 fb^{-1} of proton-proton collision data at $\sqrt{s} = 13$ TeV with the ATLAS detector. *JHEP*, 10:182, 2017.
- [4] Albert M Sirunyan et al. Search for high-mass resonances in dilepton final states in proton-proton collisions at $\sqrt{s} = 13$ TeV. *JHEP*, 06:120, 2018.
- [5] S. Amrith, J. M. Butterworth, F. F. Deppisch, W. Liu, A. Varma, and D. Yallup. LHC Constraints on a $B - L$ Gauge Model using Contur. 2018.
- [6] S. Schael et al. Fermion pair production in e^+e^- collisions at 189-209-GeV and constraints on physics beyond the standard model. *Eur. Phys. J.*, C49:411–437, 2007.
- [7] G. Abbiendi et al. Tests of the standard model and constraints on new physics from measurements of fermion pair production at 189-GeV to 209-GeV at LEP. *Eur. Phys. J.*, C33:173–212, 2004.

- [8] Ernest Ma, D. P. Roy, and Sourov Roy. Gauged $L(\mu) - L(\tau)$ with large muon anomalous magnetic moment and the bimaximal mixing of neutrinos. *Phys. Lett.*, B525:101–106, 2002.
- [9] Kento Asai, Koichi Hamaguchi, and Natsumi Nagata. Predictions for the neutrino parameters in the minimal gauged $U(1)_{L_\mu - L_\tau}$ model. *Eur. Phys. J.*, C77(11):763, 2017.
- [10] Kento Asai, Koichi Hamaguchi, Natsumi Nagata, Shih-Yen Tseng, and Koji Tsumura. Minimal Gauged $U(1)_{L_\alpha - L_\beta}$ Models Driven into a Corner. 2018.
- [11] Anirban Biswas, Sandhya Choubey, and Sarif Khan. Neutrino Mass, Dark Matter and Anomalous Magnetic Moment of Muon in a $U(1)_{L_\mu - L_\tau}$ Model. *JHEP*, 09:147, 2016.
- [12] Anirban Biswas, Sandhya Choubey, and Sarif Khan. FIMP and Muon $(g - 2)$ in a $U(1)_{L_\mu - L_\tau}$ Model. *JHEP*, 02:123, 2017.
- [13] Wolfgang Altmannshofer, Stefania Gori, Maxim Pospelov, and Itay Yavin. Neutrino Trident Production: A Powerful Probe of New Physics with Neutrino Beams. *Phys. Rev. Lett.*, 113:091801, 2014.
- [14] Francisco del Aguila, Mikael Chala, Jose Santiago, and Yasuhiro Yamamoto. Collider limits on leptophilic interactions. *JHEP*, 03:059, 2015.
- [15] Keisuke Harigaya, Takafumi Igari, Mihoko M. Nojiri, Michihisa Takeuchi, and Kazuhiro Tobe. Muon $g-2$ and LHC phenomenology in the $L_\mu - L_\tau$ gauge symmetric model. *JHEP*, 03:105, 2014.
- [16] Fatemeh Elahi and Adam Martin. Constraints on $L_\mu - L_\tau$ interactions at the LHC and beyond. *Phys. Rev.*, D93(1):015022, 2016.
- [17] Jessica Lovelace Rainbolt and Michael Schmitt. Branching fraction for Z decays to four leptons and constraints on new physics. 2018.
- [18] Albert M Sirunyan et al. Search for an $L_\mu - L_\tau$ gauge boson using $Z \rightarrow 4\mu$ events in proton-proton collisions at $\sqrt{s} = 13$ TeV. Submitted to: *Phys. Lett.*, 2018.
- [19] Manuel Drees, Herbi Dreiner, Daniel Schmeier, Jamie Tattersall, and Jong Soo Kim. CheckMATE: Confronting your Favourite New Physics Model with LHC Data. *Comput. Phys. Commun.*, 187:227–265, 2015.
- [20] Daniel Dercks, Nishita Desai, Jong Soo Kim, Krzysztof Rolbiecki, Jamie Tattersall, and Torsten Weber. CheckMATE 2: From the model to the limit. *Comput. Phys. Commun.*, 221:383–418, 2017.
- [21] J. de Favereau, C. Delaere, P. Demin, A. Giammanco, V. Lemaître, A. Mertens, and M. Selvaggi. DELPHES 3, A modular framework for fast simulation of a generic collider experiment. *JHEP*, 02:057, 2014.
- [22] S. Chatrchyan et al. The CMS Experiment at the CERN LHC. *JINST*, 3:S08004, 2008.
- [23] G. Aad et al. The ATLAS Experiment at the CERN Large Hadron Collider. *JINST*, 3:S08003, 2008.

- [24] Matteo Cacciari, Gavin P. Salam, and Gregory Soyez. FastJet User Manual. Eur. Phys. J., C72:1896, 2012.
- [25] Matteo Cacciari and Gavin P. Salam. Dispelling the N^3 myth for the k_t jet-finder. Phys. Lett., B641:57–61, 2006.
- [26] Matteo Cacciari, Gavin P. Salam, and Gregory Soyez. The anti- k_t jet clustering algorithm. JHEP, 04:063, 2008.
- [27] Alexander L. Read. Presentation of search results: The CL(s) technique. J. Phys., G28:2693–2704, 2002. [,11(2002)].
- [28] C. G. Lester and D. J. Summers. Measuring masses of semiinvisibly decaying particles pair produced at hadron colliders. Phys. Lett., B463:99–103, 1999.
- [29] Alan Barr, Christopher Lester, and P. Stephens. m(T2): The Truth behind the glamour. J. Phys., G29:2343–2363, 2003.
- [30] Hsin-Chia Cheng and Zhenyu Han. Minimal Kinematic Constraints and m(T2). JHEP, 12:063, 2008.
- [31] Yang Bai, Hsin-Chia Cheng, Jason Gallicchio, and Jiayin Gu. Stop the Top Background of the Stop Search. JHEP, 07:110, 2012.
- [32] Daniel R. Tovey. On measuring the masses of pair-produced semi-invisibly decaying particles at hadron colliders. JHEP, 04:034, 2008.
- [33] Giacomo Polesello and Daniel R. Tovey. Supersymmetric particle mass measurement with the boost-corrected contranverse mass. JHEP, 03:030, 2010.
- [34] Konstantin T. Matchev and Myeonghun Park. A General method for determining the masses of semi-invisibly decaying particles at hadron colliders. Phys. Rev. Lett., 107:061801, 2011.
- [35] Vardan Khachatryan et al. Search for a standard model-like Higgs boson in the $\mu^+\mu^-$ and e^+e^- decay channels at the LHC. Phys. Lett., B744:184–207, 2015.
- [36] Serguei Chatrchyan et al. Measurement of the W^+W^- Cross section in pp Collisions at $\sqrt{s} = 7$ TeV and Limits on Anomalous $WW\gamma$ and WWZ couplings. Eur. Phys. J., C73(10):2610, 2013.
- [37] Vardan Khachatryan et al. Measurement of the transverse momentum spectrum of the Higgs boson produced in pp collisions at $\sqrt{s} = 8$ TeV using $H \rightarrow WW$ decays. JHEP, 03:032, 2017.
- [38] Vardan Khachatryan et al. Measurement of the W^+W^- cross section in pp collisions at $\sqrt{s} = 8$ TeV and limits on anomalous gauge couplings. Eur. Phys. J., C76(7):401, 2016.
- [39] Georges Aad et al. Search for type-III Seesaw heavy leptons in pp collisions at $\sqrt{s} = 8$ TeV with the ATLAS Detector. Phys. Rev., D92(3):032001, 2015.

- [40] Albert M Sirunyan et al. Search for dark matter and unparticles in events with a Z boson and missing transverse momentum in proton-proton collisions at $\sqrt{s} = 13$ TeV. JHEP, 03:061, 2017. [Erratum: JHEP09,106(2017)].
- [41] Albert M Sirunyan et al. Search for new phenomena in final states with two opposite-charge, same-flavor leptons, jets, and missing transverse momentum in pp collisions at $\sqrt{s} = 13$ TeV. JHEP, 03:076, 2018.
- [42] A. M. Sirunyan et al. Search for new physics in events with a leptonically decaying Z boson and a large transverse momentum imbalance in proton-proton collisions at $\sqrt{s} = 13$ TeV. Eur. Phys. J., C78(4):291, 2018.
- [43] Albert M Sirunyan et al. Search for new physics in events with two soft oppositely charged leptons and missing transverse momentum in proton-proton collisions at $\sqrt{s} = 13$ TeV. Phys. Lett., B782:440–467, 2018.
- [44] A. M. Sirunyan et al. Combined search for electroweak production of charginos and neutralinos in proton-proton collisions at $\sqrt{s} = 13$ TeV. JHEP, 03:160, 2018.
- [45] Albert M. Sirunyan et al. Measurements of properties of the Higgs boson decaying to a W boson pair in pp collisions at $\sqrt{s} = 13$ TeV. Submitted to: Phys. Lett., 2018.
- [46] Albert M. Sirunyan et al. Search for supersymmetric partners of electrons and muons in proton-proton collisions at $\sqrt{s} = 13$ TeV. Submitted to: Phys. Lett., 2018.
- [47] Albert M. Sirunyan et al. Searches for pair production of charginos and top squarks in final states with two oppositely charged leptons in proton-proton collisions at $\sqrt{s} = 13$ TeV. Submitted to: JHEP, 2018.
- [48] Morad Aaboud et al. Search for electroweak production of supersymmetric particles in final states with two or three leptons at $\sqrt{s} = 13$ TeV with the ATLAS detector. 2018.
- [49] Morad Aaboud et al. Constraints on off-shell Higgs boson production and the Higgs boson total width in $ZZ \rightarrow 4\ell$ and $ZZ \rightarrow 2\ell 2\nu$ final states with the ATLAS detector. 2018.
- [50] Albert M. Sirunyan et al. Search for dark matter produced in association with a Higgs boson decaying to $\gamma\gamma$ or $\tau^+\tau^-$ at $\sqrt{s} = 13$ TeV. JHEP, 09:046, 2018.
- [51] Albert M. Sirunyan et al. Search for supersymmetry in events with a τ lepton pair and missing transverse momentum in proton-proton collisions at $\sqrt{s} = 13$ TeV. 2018.
- [52] Morad Aaboud et al. Search for additional heavy neutral Higgs and gauge bosons in the ditau final state produced in 36 fb^{-1} of pp collisions at $\sqrt{s} = 13$ TeV with the ATLAS detector. JHEP, 01:055, 2018.
- [53] Morad Aaboud et al. Search for lepton-flavor violation in different-flavor, high-mass final states in pp collisions at $\sqrt{s} = 13$ TeV with the ATLAS detector. Submitted to: Phys. Rev., 2018.
- [54] V. Khachatryan et al. A search for pair production of new light bosons decaying into muons. Phys. Lett., B752:146–168, 2016.

- [55] Albert M Sirunyan et al. Measurements of the $pp \rightarrow ZZ$ production cross section and the $Z \rightarrow 4\ell$ branching fraction, and constraints on anomalous triple gauge couplings at $\sqrt{s} = 13$ TeV. *Eur. Phys. J.*, C78:165, 2018. [Erratum: *Eur. Phys. J.*C78,no.6,515(2018)].
- [56] Albert M Sirunyan et al. Evidence for associated production of a Higgs boson with a top quark pair in final states with electrons, muons, and hadronically decaying τ leptons at $\sqrt{s} = 13$ TeV. *JHEP*, 08:066, 2018.
- [57] Morad Aaboud et al. $ZZ \rightarrow \ell^+\ell^-\ell'^+\ell'^-$ cross-section measurements and search for anomalous triple gauge couplings in 13 TeV pp collisions with the ATLAS detector. *Phys. Rev.*, D97(3):032005, 2018.
- [58] Morad Aaboud et al. Measurement of the Higgs boson coupling properties in the $H \rightarrow ZZ^* \rightarrow 4\ell$ decay channel at $\sqrt{s} = 13$ TeV with the ATLAS detector. *JHEP*, 03:095, 2018.
- [59] Morad Aaboud et al. Search for doubly charged scalar bosons decaying into same-sign W boson pairs with the ATLAS detector. Submitted to: *Eur. Phys. J.*, 2018.
- [60] Albert M Sirunyan et al. Search for an exotic decay of the Higgs boson to a pair of light pseudoscalars in the final state of two muons and two τ leptons in proton-proton collisions at $\sqrt{s} = 13$ TeV. 2018.
- [61] A. M. Sirunyan et al. Search for electroweak production of charginos and neutralinos in multilepton final states in proton-proton collisions at $\sqrt{s} = 13$ TeV. *JHEP*, 03:166, 2018.
- [62] V. Khachatryan et al. Search for light bosons in decays of the 125 GeV Higgs boson in proton-proton collisions at $\sqrt{s} = 8$ TeV. *JHEP*, 10:076, 2017.
- [63] Adam Alloul, Neil D. Christensen, CÃlline Degrande, Claude Duhr, and Benjamin Fuks. *FeynRules 2.0 - A complete toolbox for tree-level phenomenology*. *Comput. Phys. Commun.*, 185:2250–2300, 2014.
- [64] Celine Degrande, Claude Duhr, Benjamin Fuks, David Grellscheid, Olivier Mattelaer, and Thomas Reiter. *UFO - The Universal FeynRules Output*. *Comput. Phys. Commun.*, 183:1201–1214, 2012.
- [65] Johan Alwall, Michel Herquet, Fabio Maltoni, Olivier Mattelaer, and Tim Stelzer. *Madgraph 5: going beyond*. *Journal of High Energy Physics*, 2011(6):1–40, 2011.
- [66] Torbjörn Sjöstrand, Stefan Ask, Jesper R Christiansen, Richard Corke, Nishita Desai, Philip Ilten, Stephen Mrenna, Stefan Prestel, Christine O Rasmussen, and Peter Z Skands. *An introduction to pythia 8.2*. *Computer Physics Communications*, 191:159–177, 2015.
- [67] Fred Jegerlehner and Andreas Nyffeler. *The Muon g-2*. *Phys. Rept.*, 477:1–110, 2009.
- [68] S. R. Mishra et al. Neutrino tridents and WZ interference. *Phys. Rev. Lett.*, 66:3117–3120, 1991.
- [69] D. Geiregat et al. First observation of neutrino trident production. *Phys. Lett.*, B245:271–275, 1990.

- [70] J. P. Lees et al. Search for a muonic dark force at BABAR. *Phys. Rev.*, D94(1):011102, 2016.
- [71] Eung Jin Chun, Arindam Das, Jinsu Kim, and Jongkuk Kim. Searching for Flavored Gauge Bosons. 2018.
- [72] S. Agostinelli et al. GEANT4: A Simulation toolkit. *Nucl. Instrum. Meth.*, A506:250–303, 2003.